Eur. Phys. J. C (2017) 77:371
DOI 10.1140/epjc/s10052-017-4951-1

THE EUROPEAN PHYSICAL JOURNAL C

Regular Article - Theoretical Physics

Uncover compressed supersymmetry via boosted bosons from the heavier stop/sbottom

Zhaofeng Kang[1,a], **Jinmian Li**[1,b], **Mengchao Zhang**[2,c]

[1] School of Physics, Korea Institute for Advanced Study, Seoul 130-722, Korea
[2] Center for Theoretical Physics of the Universe, Institute for Basic Science (IBS), Daejeon 34051, Korea

Received: 31 March 2017 / Accepted: 28 May 2017

Abstract A light stop around the weak scale is a hopeful messenger of natural supersymmetry (SUSY), but it has not shown up at the current stage of LHC. Such a situation raises the question of the fate of natural SUSY. Actually, a relatively light stop can easily be hidden in a compressed spectra such as mild mass degeneracy between stop and neutralino plus top quark. Searching for such a stop at the LHC is a challenge. On the other hand, in terms of the argument of natural SUSY, other members in the stop sector, including a heavier stop $\tilde{t}_2$ and lighter sbottom $\tilde{b}_1$ (both assumed to be left-handed-like), are also supposed to be relatively light and therefore searching for them would provide an alternative method to probe natural SUSY with a compressed spectra. In this paper we consider quasi-natural SUSY which tolerates relatively heavy colored partners near the TeV scale, with a moderately large mass gap between the heavier members and the lightest stop. Then $W/Z/h$ as companions of $\tilde{t}_2$ and $\tilde{b}_1$ decaying into $\tilde{t}_1$ generically are well boosted, and they, along with other visible particles from $\tilde{t}_1$ decay, are a good probe to study compressed SUSY. We find that the resulting search strategy with boosted bosons can have better sensitivity than those utilizing multi-leptons.

1 Introduction

Supersymmetry (SUSY), devised to elegantly solve the gauge hierarchy problem, used to and will provide the major impetus for building high energy colliders, such as the LHC. Guided by the naturalness argument [1–4], stops, among a bunch of new particles predicted by SUSY, should be light and therefore, along with their color charges, may furnish the first "smoking-gun" signature for SUSY at the LHC.

Nevertheless, confirmatory hints for light stops at the LHC are absent so far. Considering that the LHC is now already running at the CM energy $\sqrt{s} = 13\,\text{TeV}$, the null results arouse concerns about the existence of low energy SUSY, or more concretely a light stop below the TeV scale. Actually, the current LHC search strategies [5–12] still leave a wide room for a relatively light stop ($\sim$500 GeV), provided that a very large missing energy from stop decay is not present, say due to a compressed spectrum. Such a spectrum is characterized by very close mass between stop $\tilde{t}$ and the lightest sparticle (LSP) [13–38], or more loosely speaking $m_{\tilde{t}} \sim m_t + m_{\text{LSP}}$ and $m_{\tilde{t}} \sim m_b + m_W + m_{\text{LSP}}$.[1] Despite allowing for a natural low energy supersymmetry, it is challenging to uncover such a stop at the LHC. Nevertheless, if naturalness is reliable, the heavier stop and the lighter sbottom should not lie far above $m_{\tilde{t}_1}$, thus being detectable. This motivates the searches for the signal of $\tilde{t}_2$ pair production with $\tilde{t}_2 \to \tilde{t}_1 h/Z$ decay at the LHC run-I [40,41]. Moreover, through searching for the final state of multi-leptons and/or multi-b-jets [42], the heavier stop/sbottom with masses below $\sim$ 1 TeV decaying into $\tilde{t}_1$ and heavy bosons are found to be detectable at the 13/14 TeV LHC with an integrated luminosity of $\mathcal{O}(100)\,\text{fb}^{-1}$ [43–46].

On the other hand, boosted objects such as a boosted top quark, vector bosons and the Higgs boson being new physics signatures have been receiving increasing experimental attention [47–50], where the new physics scale is pushed into the higher and higher region. The substructures of these boosted objects furnish a powerful tool to distinguish the signatures from the huge QCD backgrounds. Taking into account that they (top etc.) dominantly decay into hadrons, the substructure approach may be more efficient than the searching approach utilizing their leptonic final

[a] e-mail: zhaofengkang@gmail.com
[b] e-mail: jmli@kias.re.kr
[c] e-mail: mczhang@ibs.re.kr

[1] In the case of a sneutrino LSP, the compressed spectrum may require $m_{\tilde{t}_1} \approx m_t + \ell + m_{\tilde{\nu}_1}$ [39], where three-body can help to soften missing energy even the compression is only mild.

Published online: 05 June 2017

states. This leads us to reconsider the strategy of searching for the heavier stop/sbottom in the compressed SUSY scenario. If there is a relatively large mass splitting between the heavier stop/sbottom ($\tilde{t}_2/\tilde{b}_1$) and the lighter stop ($\tilde{t}_1$), the $h/Z/W$ boson in the decay chain $\tilde{t}_2 \to h/Z\tilde{t}_1$ and $\tilde{b}_1 \to W\tilde{t}_1$ will be quite energetic. Hence, hunting for $\tilde{t}_2/\tilde{b}_1$ by tagging these boosted bosons may be a promising way. It was already tried in an earlier paper [51], which employed the boosted boson tag technique to probe the highly mixed stop sector and obtained a satisfactory sensitivity for $m_{\tilde{t}_2} \sim 1$ TeV and $m_{\tilde{t}_1} \sim 400$ GeV. But this study focused on the case of degeneracy between $\tilde{t}_1$ and the LSP, with $m_{\tilde{t}_1} - m_{\tilde{\chi}_1^0} \sim \mathcal{O}(10)$ GeV, which requires the flavor-violating decay $\tilde{t}_1 \to c\tilde{\chi}_1^0$ and renders $\tilde{t}_1$ invisible. Whereas for the moderately compressed spectrum considered in this paper, additional visible particles from $\tilde{t}_1$ (flavor conserving) decay are available.

So, in this paper we consider a (simplified) quasi-natural pattern of low energy supersymmetry where the lighter stop of a few hundred GeV is right-handed stop like and lives in the compressed regions, due to its close mass with bino or Higgsinos; whereas states in the doublet $\tilde{Q}_3$ are around the TeV scale. Thus, the characteristic signatures of this model contain fairly boosted bosons from decays $\tilde{Q}_3 \to \tilde{t}_1 + W/Z/h$. To demonstrate the prospects of those signatures at the LHC, we choose four benchmark points corresponding to four possible decay modes of $\tilde{t}_1$: (1) $\tilde{t}_1 \to b\tilde{\chi}_1^{\pm}$; (2) $\tilde{t}_1 \to bff\tilde{\chi}_1^0$; (3) $\tilde{t}_1 \to bW\tilde{\chi}_1^0$; (4) $\tilde{t}_1 \to t\tilde{\chi}_1^0$, which produce extra detectable b-jets and leptons as well as missing transverse energy (MET). Therefore, boosted bosons plus MET, associated with b-jets/leptons constitute the smoking-gun signature for such a compressed SUSY. By adopting the boosted decision tree (BDT) method for signal and background discrimination, we find that the resulting search strategy with boosted bosons can have better sensitivity than those utilizing multi-leptons.

The paper is organized as the following. In Sect. 2 we establish the quasi-natural SUSY which can hide the lighter stop involving the minimal degrees of freedom and demonstrate the distribution of $\tilde{t}_2$ and $\tilde{b}_1$ decays in the MSSM. In Sect. 3 we detail the signal and background analysis at the LHC. Discussions and conclusions are presented in the final section.

2 Quasi-natural supersymmetry

In this section we will present the quasi-natural model with minimal field content and analyze the decay modes of the heavier stop and sbottom, in particular the bosonic modes, analytically and numerically. Accordingly, benchmark points are selected.

2.1 A minimal setup

Asides from a light stop sector, naturalness arguments in general favor a weak scale μ-term, thus light Higgsinos. On the other hand, considering the SUSY status after the discovery of a relatively heavy SM-like Higgs boson but there being no hints for light stops, we may have to abandon the ideal naturalness criterion and tolerate fine-tuning to some degree, say 1% or even worse [52,53]. Such a situation inspires us to consider a quasi-natural SUSY involving a minimal set of particles that accommodate a light stop $\tilde{t}_1$ with or without weak scale Higgsinos; other superpartners, including $\tilde{b}_R$ and winos, are simply assumed to decouple for simplicity. The resulting Lagrangian most relevant to our discussions derived from the flavor basis is (we just schematically list the terms).[2]

$$\begin{aligned} -\mathcal{L}_{QNS} = {} & m_{\tilde{Q}_3}^2 |\tilde{Q}_3|^2 + \frac{m_{\tilde{B}}}{2}\tilde{B}\tilde{B} + m_{\tilde{t}_R}^2 |\tilde{t}_R|^2 \\ & + \left(h_t A_t \tilde{Q}_3 H_u t_R^{\dagger} + |D_\mu \tilde{Q}_3|^2\right) \\ & + i\sqrt{2}\left(\frac{g_Y}{6}\tilde{Q}_3^{\dagger}\tilde{B}t_L - \frac{2g_Y}{3}\tilde{t}_R^{\dagger}\tilde{B}t_R\right) \\ & + \left(\mu \tilde{H}_u \tilde{H}_d + h_t \tilde{Q}_3 \tilde{H}_u t_R^{\dagger} + h_b \tilde{Q}_3 \tilde{H}_d b_R^{\dagger}\right) + \text{h.c.}, \end{aligned} \tag{2.1}$$

where $D_\mu = \partial - i\frac{g_2}{\sqrt{2}}\left(T^+ W_\mu^+ + T^- W_\mu^-\right) - i\frac{g_2}{\cos\theta_W} Z_\mu \left(T^3 - \sin^2\theta_W Q\right) + \ldots$ with θ_W the Weinberg mixing angle. In the second line, terms in the first and second brackets may be irrelevant if $\tilde{B}$ and μ are much heavier than all other particles therein, respectively. For simplicity, we will consider that either the bino or the Higgsino is light and might provide the LSP. Although a large A_t is not necessarily required in this setup, we will see that it is crucial viewing things in the perspective of collider searches; besides, recalling the difficulty in achieving a relatively heavy SM-like Higgs boson in natural SUSY, a large A_t, which could really help to radiatively enhance the Higgs boson mass, is well motivated. A good case in point of such a kind of quasi-natural SUSY is the Higgs deflected gauge mediated SUSY-breaking [54].

A compressed superpartner spectrum could make $\tilde{t}_1$ hard to detect. If the mass degeneracy between $\tilde{t}_1$ and LSP is mild and $\tilde{t}_1 \to t + \tilde{\chi}_1^0$ or $b + \tilde{\chi}_1^{\pm}$ is kinematically accessible, they will become the main decay modes of $\tilde{t}_1$. If degeneracy becomes severer, the above channels are closed and $\tilde{t}_1$ will dominantly have three- (four)-body decays into $bW^{(*)}\tilde{\chi}_1^0$, assuming that the flavor changing decay $\tilde{t}_1 \to c\tilde{\chi}_1^0$, which strongly depends on the unknown flavor structure of squarks,

[2] We do not consider the way to obtain a 125 GeV SM-like Higgs boson mass in this paper; other sources of Higgs mass should be introduced, otherwise the stop sector will be pushed into the multi-TeV region and be almost inaccessible at the LHC.

is negligible. As a matter of fact, the four-body decay case is particularly well motivated after identifying the bino as the dark matter candidate: the bino is a gauge singlet, so, in order to reduce its relic density during the freeze-out era, usually coannihilation with a nearly degenerate stop is necessary; for a sub TeV bino DM, a fairly small mass difference $m_{\tilde{t}_1} - m_{\tilde{\chi}_1^0} \sim 30\,\text{GeV}$ is needed [55].

To hide a light $\tilde{t}_1$ at the current LHC, it is better to let $\tilde{t}_1$ dominantly reside in $\tilde{t}_R$; otherwise, the accompanying $\tilde{b}_L$, which has close mass with $\tilde{t}_1 \approx \tilde{t}_L$, would have been uncovered via $\tilde{b}_L \to \tilde{\chi}_1^0 b$ except for the highly degeneracy between $\tilde{t}_1$ and $\tilde{\chi}_1^0$, a case that has been extensively discussed before [45]. Moreover, in this paper we focus on the doublet $\tilde{Q}_3 = (\tilde{b}_L, \tilde{t}_L)$ being considerably heavier than $\tilde{t}_R \approx \tilde{t}_1$, and therefore, by tagging the boosted bosons from $\tilde{Q}_3$ decaying into $\tilde{t}_1$, they may show a more promising prospect at the LHC than $\tilde{t}_1$, which is somewhat hidden as before. On the contrary, $\tilde{Q}_3$ having similar mass to $\tilde{t}_1$ may be hard to discover, because their decay final states typically are soft. In this sense the heavier stop/sbottom may instead provide the smoking gun for (quasi-)natural SUSY.

2.2 Bosonic decay modes of $\tilde{t}_2$ and $\tilde{b}_1$: roles of a large A_t

In this section, we examine the bosonic decay modes of $\tilde{t}_2$ and $\tilde{b}_1$ and see the conditions which make them the dominant modes. These decays do not depend on the nature of LSP. Concretely, their decay widths are given by [56]

$$\begin{aligned}
\Gamma(\tilde{b}_1 \to \tilde{t}_1 W) &\approx \frac{g_2^2 \cos^2\theta_{\tilde{t}}}{32\pi} \frac{m_{\tilde{b}_1}^3}{m_W^2} \lambda^{3/2}(m_{\tilde{b}_1}^2, m_{\tilde{t}_1}^2, m_W^2),\\
\Gamma(\tilde{t}_2 \to \tilde{t}_1 Z) &\approx \frac{g_2^2}{\cos^2\theta_W} \frac{\sin^2 2\theta_{\tilde{t}}}{256\pi} \frac{m_{\tilde{t}_2}^3}{m_Z^2} \lambda^{3/2}(m_{\tilde{t}_2}^2, m_{\tilde{t}_1}^2, m_Z^2),\\
\Gamma(\tilde{t}_2 \to \tilde{t}_1 h) &\approx \frac{g_2^2 \cos^2 2\theta_{\tilde{t}}}{64\pi} \frac{m_t^2}{m_W^2} \frac{A_t^2}{m_{\tilde{t}_2}} \lambda^{1/2}(m_{\tilde{t}_2}^2, m_{\tilde{t}_1}^2, m_h^2),
\end{aligned} \tag{2.2}$$

with $\lambda(a,b,c) = [1-(b+c)/a]^2 - 4bc/a^2 \approx 1$. We have taken $h \sim \text{Re}(H_u^0)$ to get the last expression. Here $\tilde{\theta}_t$ is the mixing angle between the left- and right-handed stops, defined through

$$\tilde{t}_L = \cos\theta_{\tilde{t}}\tilde{t}_1 - \sin\theta_{\tilde{t}}\tilde{t}_2, \quad \tilde{t}_R = \sin\theta_{\tilde{t}}\tilde{t}_1 + \cos\theta_{\tilde{t}}\tilde{t}_2, \tag{2.3}$$

and $\tan 2\theta_{\tilde{t}} = 2X_t m_t/(m_{\tilde{Q}_3}^2 - m_{\tilde{t}_R}^2)$ with $X_t = A_t + \mu/\tan\beta$. If $\tilde{t}_1$ is very $\tilde{t}_R$-like, one will have $\tilde{\theta}_t \to \pi/2$ and consequently all the bosonic modes except for $\tilde{t}_2 \to \tilde{t}_1 h$ will be highly suppressed. A large A_t is thus indispensable: It does not only generate sizable LR stop mixing but also directly enhances $\tilde{t}_2 \to \tilde{t}_1 h$.[3] In practice, we do not need a fairly sizable $\theta_{\tilde{t}}$ because the (longitudinal) W/Z modes are enhanced by a factor like $\left(m_{\tilde{t}_2}/m_Z\right)^2 \sim \mathcal{O}(10^2)$ for a TeV scale $m_{\tilde{Q}_3}$, which could easily compensate the mild suppression from the small mixing.

Now we analyze their heavy quark decay modes based on the quasi-natural SUSY, see Eq. (2.1), which are sensitive to the LSP components. In the most general cases, the decay widths take the forms of [56]

$$\begin{aligned}
\Gamma(\tilde{q}_i \to q\tilde{\chi}_k^0) &= \frac{g_2^2}{16\pi m_{\tilde{q}_i}}\\
&\times \left[\left((h_{ik}^q)^2 + (f_{ik}^q)^2\right)\left(m_{\tilde{q}_i}^2 - m_q^2 - m_{\tilde{\chi}_k^0}^2\right) - 4h_{ik}^q f_{ik}^q m_q m_{\tilde{\chi}_k^0}\right],
\end{aligned} \tag{2.4}$$

$$\begin{aligned}
\Gamma(\tilde{q}_i \to q'\tilde{\chi}_k^\pm) &= \frac{g_2^2}{16\pi m_{\tilde{q}_i}}\\
&\times \left[\left((l_{ik}^{\tilde{q}})^2 + (k_{ik}^{\tilde{q}})^2\right)\left(m_{\tilde{q}_i}^2 - m_{q'}^2 - m_{\tilde{\chi}_k^0}^2\right) - 4l_{ik}^{\tilde{q}} k_{ik}^{\tilde{q}} m_{q'} m_{\tilde{\chi}_k^\pm}\right],
\end{aligned} \tag{2.5}$$

where $\tilde{q}_i$ denote $\tilde{t}_{1,2}$ and $\tilde{b}_1$. The matrices h_{ik}^q etc. encode couplings between quark and squark, neutralinos; in the following we will give their concrete expressions in the Higgsino- and bino-LSP limits.

We first consider the Higgsinos to be light, while the bino can be dropped; moreover, we will use the strip $m_b + |\mu| < m_{\tilde{t}_1} \lesssim m_t + |\mu|$ to hide $\tilde{t}_1$. In the limit of a left-handed sbottom, while we have the right-handed light stop, namely $\theta_{\tilde{t}} \to \pi/2$, and a Higgsino LSP (actually two with almost degenerate masses involved), one obtains

$$\begin{aligned}
&h_{21}^t \approx h_{22}^t \approx 0, \quad |f_{21}^t| \approx |f_{22}^t| \approx \frac{m_t}{2m_W}\sin\theta_{\tilde{t}},\\
&|h_{11}^b| \approx |h_{12}^b| \approx \frac{m_b}{2m_W}\tan\beta, \quad f_{11}^b \approx f_{12}^b \approx 0,
\end{aligned} \tag{2.6}$$

$$\begin{aligned}
&l_{21}^{\tilde{t}} \approx 0, \quad |k_{21}^{\tilde{t}}| \approx \frac{m_b}{\sqrt{2}m_W\cos\beta}\sin\theta_{\tilde{t}},\\
&l_{11}^{\tilde{b}} \approx 0, \quad |k_{11}^{\tilde{b}}| \approx \frac{m_t}{\sqrt{2}m_W\sin\beta},
\end{aligned} \tag{2.7}$$

where a relatively large $\tan\beta$ at least is assumed. Next we move to the other case where the Higgsinos are decoupled and the bino is the LSP. In this case a lighter $\tilde{t}_1$ is allowed if its mass does not significantly exceed $m_t + m_{\tilde{\chi}_1^0}$. Now the couplings are reduced to

$$|h_{21}^t| \approx \frac{2\sqrt{2}}{3}\sin\theta_W\sin\theta_{\tilde{t}}, \quad |f_{11}^b| \approx \frac{\sqrt{2}}{3}\sin\theta_W\sin\theta_{\tilde{t}}. \tag{2.8}$$

[3] In Ref. [57], assuming that $\tilde{t}_1$ behaves like a pure missing energy at the LHC, say in the highly compressed limit, a new search approach based on boosted di-Higgs plus missing energy was proposed.

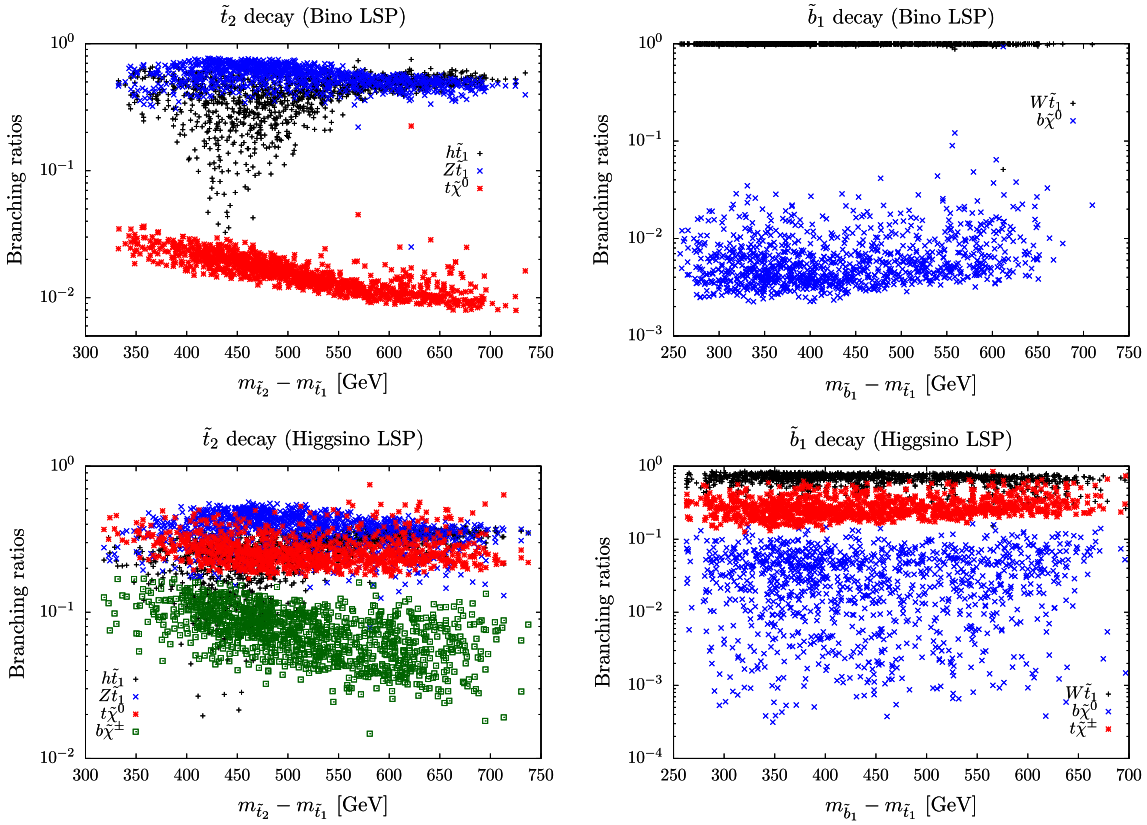

Fig. 1 $\tilde{t}_2$ (*left panels*) and $\tilde{b}_1$ (*right panels*) decay branching ratios for bino LSP (*upper panel*) and Higgsino LSP (*lower panels*)

All others are suppressed by small mixing angles, and they thus are of no importance. Moreover, since the charginos are decoupled, here we do not need to consider $l^{\tilde{b}}_{1j}$, etc.

We would like to stress that, in the bino-LSP, case the decay modes of $\tilde{t}_2$ and $\tilde{b}_1$ into the heavy flavors, such as $\tilde{t}_2 \to t + \tilde{\chi}^0_1$ and $\tilde{b}_1 \to b + \tilde{\chi}^0_1$, are substantially suppressed, because now they come from hypercharge gauge interactions rather than the y_t-Yukawa interaction as in the light Higgsino case. One can clearly see this situation from Fig. 1, which shows that those branching ratios typically are below $\mathcal{O}(1\%)$ in the bino LSP scenario. Such a situation makes good for the more boosted bosons from $\tilde{t}_2/\tilde{b}_1$ decay. But even in the Higgsino LSP case, for a heavier $m_{\tilde{Q}_3}$ with a large A_t coupling, these bosonic modes generically have quite sizable branching ratios, $\gtrsim\mathcal{O}(10\%)$, by virtue of the significant Goldstone enhancement factor stressed before. In particular, $\tilde{b}_1$, which has less decay modes than $\tilde{t}_2$, almost dominantly decays into W plus $\tilde{t}_1$ in both cases. It can be understood from the estimation (in the Higgsino-LSP limit):

$$\frac{\Gamma(\tilde{b}_1 \to W\tilde{\chi}^\pm_1)}{\Gamma(\tilde{b}_1 \to b\tilde{\chi}^0_1)} \simeq \left(\frac{m_{\tilde{b}_1}}{m_t}\right)^2 \cos^2\theta_{\tilde{t}} \gtrsim \frac{A_t^2}{m^2_{\tilde{Q}_3}}. \tag{2.9}$$

In the next section, we will choose several benchmarks points to embody the above possible scenarios for quasi-natural SUSY.

2.3 Decay patterns in quasi-natural SUSY: scanning results and benchmark points

For concreteness, we implement quasi-natural SUSY in the minimal supersymmetric SM (MSSM). There are totally five parameters of interests in each scenario with either decoupled bino or Higgsino. We use Suspect2 [58] and SUSY-HIT [59] to calculate the mass spectrum and the decay branching ratios of stops and sbottom. The parameter scan is performed in the following range:

$$\begin{aligned} &m_{\tilde{Q}_3} \in [700, 1200]\ \text{GeV}, \quad m_{\tilde{U}_3} \in [500, 700]\ \text{GeV}, \\ &|A_t| \in [1, 3]\ \text{TeV}, \quad \tan\beta \in [3, 50], \\ &\mu \in [300, 700]\ \text{GeV}\ (M_1 = 2\ \text{TeV})\ \text{or} \\ &M_1 \in [300, 700]\ \text{GeV}\ (\mu = 2\ \text{TeV}). \end{aligned} \tag{2.10}$$

The rest of the soft mass parameters of the MSSM are set to 2 TeV, so those sparticles are decoupled from the mass spectrum. The choice of the above parameter pattern is motivated by the non-detection of any stop/sbottom signals at the current stage of LHC [5–12]; the resulting spectrum still

Table 1 Benchmark points for different decay modes of the right-handed dominant $\tilde{t}_1$. $\mathrm{Br}(\tilde{t}_1 \to bW^{(*)}\tilde{\chi}_1^0)$ of T14B (1000) is slightly smaller than one because the flavor changing decay $\tilde{t}_1 \to c\tilde{\chi}_1^0$ is also important here

	$m_{\tilde{t}_2/\tilde{b}_1} \sim 800\,\mathrm{GeV}$				$m_{\tilde{t}_2/\tilde{b}_1} \sim 1000\,\mathrm{GeV}$			
	T1BC	T14B	T1BW	T1TN	T1BC	T14B	T1BW	T1TN
M_1 (GeV)	2000	450	380	340	2000	429	370	330
μ (GeV)	470	2000	2000	2000	470	2000	2000	2000
$\tan\beta$	3.0	3.0	3.0	3.0	3.0	5.0	5.0	5.0
$m_{\tilde{Q}_3}$ (GeV)	830	870	870	870	1000	1000	1000	1000
$m_{\tilde{U}_3}$ (GeV)	650	620	620	620	650	630	630	630
A_t (GeV)	1000	1000	1000	1000	1000	−1000	−1000	−1000
$m_{\tilde{t}_1}$ (GeV)	518	533	533	533	574	517	517	517
$m_{\tilde{t}_2}$ (GeV)	810	826	826	826	993	984	984	984
$m_{\tilde{b}_1}$ (GeV)	774	821	821	821	977	968	968	968
$m_{\tilde{\chi}_1^0}$ (GeV)	470	454	383	343	471	434	374	334
$m_{\tilde{\chi}_2^0}$ (GeV)	475	2000	2000	2000	476	2000	2000	2000
$m_{\tilde{\chi}_1^\pm}$ (GeV)	472	2000	2000	2000	472	2000	2000	2000
$\mathrm{Br}(\tilde{t}_2 \to h\tilde{t}_1)$	0.163	0.399	0.393	0.389	0.204	0.502	0.501	0.500
$\mathrm{Br}(\tilde{t}_2 \to Z\tilde{t}_1)$	0.330	0.526	0.518	0.514	0.219	0.486	0.485	0.484
$\mathrm{Br}(\tilde{b}_1 \to W\tilde{t}_1)$	0.621	0.963	0.954	0.949	0.431	0.988	0.987	0.986
$\mathrm{Br}(\tilde{t}_1 \to b\tilde{\chi}_1^\pm)$	1.0	0	0	0	1.0	0	0	0
$\mathrm{Br}(\tilde{t}_1 \to bW^{(*)}\tilde{\chi}_1^0)$	0	1.0	1.0	0	0	0.882	1.0	0
$\mathrm{Br}(\tilde{t}_1 \to t\tilde{\chi}_1^0)$	0	0	0	1.0	0	0	0	1.0

allows a light stop with mass ∼500 GeV if the LSP is relatively heavy ($m_{\mathrm{LSP}} \gtrsim 300\,\mathrm{GeV}$). Moreover, we require the mass of the heavier stop and the sbottom to be around the TeV scale to produce relatively boosted bosons in their decay, while still having sizable production rates for discovery in the near future. We note that the searches for a heavier stop at the LHC run-I [40,41] are only able to exclude models with $m_{\tilde{t}_2} \lesssim 600\,\mathrm{GeV}$. As we have discussed in Sect. 2.2, a sizable $|A_t|$ is needed to enhance $\mathrm{Br}(\tilde{t}_2 \to h\tilde{t}_1)$ and $\mathrm{Br}(\tilde{t}_2 \to Z\tilde{t}_1)$, so a lower limit of $|A_t|$ is set to improve the scanning efficiency. Since we are expecting new contributions other from the stop in MSSM to the Higgs boson mass, the lighter CP-even Higgs boson ($H_1 \equiv h$) mass is set to 125 GeV manually when calculating the decay branching ratios. The heavier CP-even Higgs (H_2) is decoupled by setting $m_A = 2$ TeV.

In Fig. 1, we plot the decay branching ratios of the heavier stop ($\tilde{t}_2$) and the lighter sbottom ($\tilde{b}_1$) for either bino LSP or Higgsino LSP. In the upper panels where the bino is the LSP, we can see that the bosonic modes dominate the stop/sbttom decay in the full parameter space, while the branching fractions of the $\tilde{t}_2 \to t\tilde{\chi}_1^0/\tilde{b}_1 \to b\tilde{\chi}_1^0$ modes typically are two orders of magnitude smaller. The situation changes when Higgsino is the LSP. In the lower panels, decay widths of $\tilde{t}_2 \to t\tilde{\chi}_1^0/\tilde{b}_1 \to b\tilde{\chi}_1^0$, which are enhanced by the larger top quark Yukawa coupling, become comparable with that of the bosonic modes. Moreover, there will be new decay modes opening due to the charged Higgsino in the final state, i.e., $\tilde{t}_2 \to b\tilde{\chi}_1^\pm$ and $\tilde{b}_1 \to t\tilde{\chi}_1^\pm$, whose branching fractions are also sizable. Nevertheless, we can observe that the bosonic mode is still one of the dominant decay modes for both $\tilde{t}_2$ and $\tilde{b}_1$.

In terms of the scanning results, eight benchmark points are chosen to illustrate the model details in Table 1, which are featured by the different decay modes of the lighter stop, as well as two choices of the $\tilde{t}_2/\tilde{b}_1$ masses, that is, $m_{\tilde{t}_2/\tilde{b}_1} \sim 800\,\mathrm{GeV}$ and $m_{\tilde{t}_2/\tilde{b}_1} \sim 1000\,\mathrm{GeV}$, respectively. These differences will be used to label each benchmark point in the following discussions, e.g., T1BC (800) corresponding to the one which has $m_{\tilde{t}_2/\tilde{b}_1} \sim 800\,\mathrm{GeV}$ along with a lighter stop mainly decaying into $b + \tilde{\chi}_1^0$.

3 Collider phenomenology

3.1 Search strategy

For all benchmark points, the left-handed-like $\tilde{t}_2$ and $\tilde{b}_1$ have similar masses, both dominantly decaying into a gauge boson/Higgs boson plus the lighter stop $\tilde{t}_1$. The high multiplicity of gauge bosons in the final state will lead to multiple leptons events. Moreover, one would expect two bottom quark jets in the final state if the flavor changing decay of $\tilde{t}_1 \to c\tilde{\chi}_1^0$ is suppressed. Studies [40,41,43,44,46] have shown that searching for final states with leptons and b-

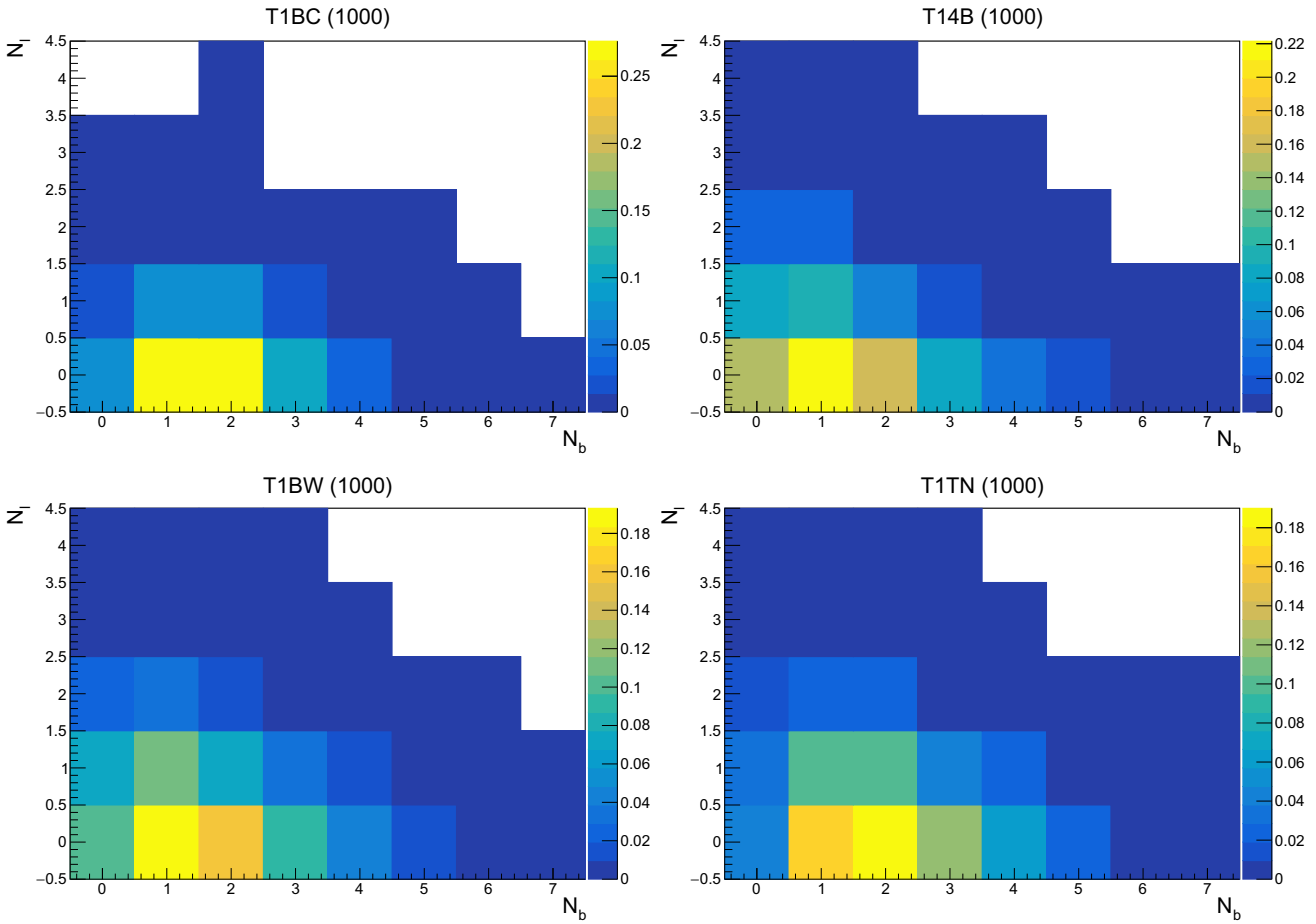

Fig. 2 The number of b-jets N_b and the number of leptons N_ℓ distributions for our benchmark points with $m_{\tilde{t}_L}$=1 TeV

jets provides as a good probe to study the light stop sector, especially when $m_{\tilde{t}_1} \sim m_t + m_{\tilde{\chi}_1^0}$. However, for some of our benchmark points, e.g. T14B, the small mass difference between $m_{\tilde{t}_1}$ and $m_{\tilde{\chi}_1^0}$ may render the b-jets/leptons undetectable.

To see the point more clearly, we generate the parton level events for our benchmark points with MadGraph5 [60], which are passed to Pythia6 [61] for particle decay, parton showering and hadronization. The Delphes3 [62] with input of the default ATLAS detector card is used for simulating detector effects. In this work, we take the b-jet tagging efficiency as 70%, with the other light quark and gluon mistagging probability 1% [63].

We consider the signals of both $\tilde{t}_2$ and $\tilde{b}_1$ pair production with subsequent decays for benchmark points with $m_{\tilde{t}_L}$=1 TeV. The corresponding N_b versus N_ℓ distributions are given in Fig. 2. It can be seen that even for the benchmark point T1TN, in which $\tilde{t}_1$ dominantly decays into $t\tilde{\chi}_1^0$, only around 20% of the total events contain at least one b-jet and one lepton. The fraction becomes even smaller for other benchmark points owing to the heavier $\tilde{\chi}_1^0$. Events with b-jet multiplicity higher than 2 originate from $h_{\rm SM} \to b\bar{b}$. In all cases, we find that the fraction of events with $N_l \geq 2$ is at the percent level. Consequently, despite relatively low backgrounds, searching for final states with multiple leptons is suffering from serious branching ratio suppressions in the signal processes.

On the other hand, signals with hadronic decaying bosons from $\tilde{t}_2/\tilde{b}_1$ decay have much larger production rates. Moreover, some recent developments in the jet substructure analysis [47,50,64,65] are found to be very useful in suppressing hadronic SM backgrounds in the boosted region. Because of the relatively large mass splitting between $\tilde{t}_2/\tilde{b}_1$ and $\tilde{t}_1$, the $h/Z/W$ bosons from the heavier squarks decay usually are well boosted. Considering the $\tilde{t}_2 \to Z\tilde{t}_1$ process as an example and taking $m_{\tilde{t}_1} = 500\,\text{GeV}$, we plot parton level distributions of the transverse momentum of the Z boson and the angular distance between two fermions from Z decay in Fig. 3. We can see from the figure that the typical transverse momentum of the Z boson exceeds $\sim 150\ (200)\,\text{GeV}$, while the angular distance between the Z boson decay products $\Delta R(f, f)$ which is roughly proportional to $2m_Z/p_T(Z)$, typically is less than $\sim$1.5 (1.0) for $m_{\tilde{t}_2} = 800\ (1000)\,\text{GeV}$.

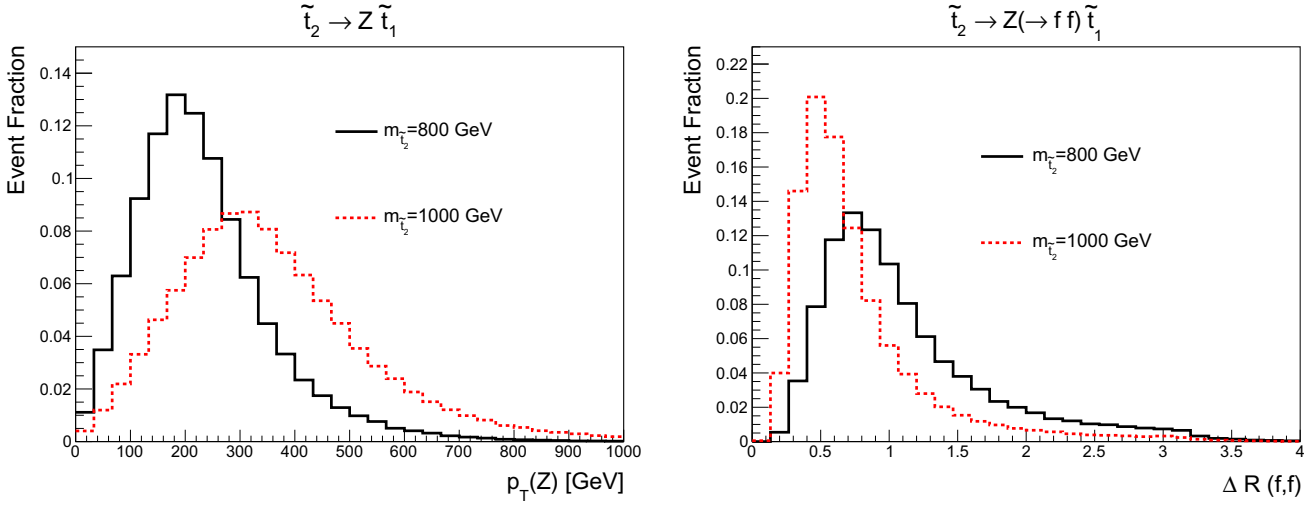

Fig. 3 *Left* the transverse momentum distribution for the Z boson in $\tilde{t}_2 \to Z\tilde{t}_1$, taking $m_{\tilde{t}_1} = 500$ GeV and $m_{\tilde{t}_2} = 800/1000$ GeV. *Right* the angular distance $\Delta R = \sqrt{(\Delta\phi)^2 + (\Delta\eta)^2}$ between the two fermions from the Z boson decay

The closeness of the Z boson decay products indicates that they can be reconstructed as a whole, i.e., as a boson jet. A boson jet which has high invariant mass and appropriate substructure can be distinguished from QCD jet, thus providing a most important handle for searching our benchmark points. Besides, there will be extra activities from the subsequent lighter stop $\tilde{t}_1$ decay, such as leptons and b-jets. In the following, we propose a search for the final state with two boson jets alongside with extra leptons/b-jets.

3.2 Signal and background analysis

The signal processes that we are aiming to search for are

$$p\,p \to \tilde{t}_2\,\bar{\tilde{t}}_2, \quad \tilde{t}_2 \to h/Z\,\tilde{t}_1, \tag{3.1}$$

$$p\,p \to \tilde{b}_1\,\bar{\tilde{b}}_1, \quad \tilde{b}_1 \to W\,\tilde{t}_1, \tag{3.2}$$

with decay branching fractions of $\tilde{t}_2$, $\tilde{b}_1$ and $\tilde{t}_1$ given in Table 1. At the LHC, the signal events can be trigged by requiring a large missing transverse momentum in the final state, $\not{E}_T > 200$ GeV. As for event reconstruction, we first identify isolated electrons and muons with $p_T(e,\mu) > 10$ GeV and $|\eta(e,\mu)| < 2.5$, where the isolation means that the scalar sum of transverse momenta of all particles with $p_T > 0.5$ GeV that lie within a cone of radius $R = 0.5$ around the $e(\mu)$ is less than 12%(25%) of the transverse momentum of $e(\mu)$. Next, tracks that do not belong to isolated leptons as well as neutral particles are used for jet clustering with fastjet [66]. We adopt the BDRS method [47] for tagging boosted boson jets: (1) reconstructing the boson jet candidates (fat jet) using C/A algorithm [67] with radius $R = 1.2$ and $p_T > 150$ GeV; (2) breaking each fat jet by undoing the clustering procedure. The two boson jets (V_1, V_2) are taken as the two leading fat jets with highest transverse momenta that have large mass dropping to $\mu < 0.67$ and we have a not too asymmetric mass splitting $y > 0.09$ at any step during the declustering; (3) filtering each of the boson jets neighborhood by rerunning the C/A algorithm with a finer angle $R_{\rm filt} = \min(0.3, R_{j_1,j_2}/2)$ and taking the three hardest subjets; (4) applying a b-tag on the two leading subjets, where we have followed the b-tagging method that is used in Delphes: identifying the hadronic jet as the generated quark with largest PDG number that lies within the distance of $\Delta R < R_{\rm filt}$ of the jet axis. The probabilities of b-tagging a b-jet, c-jet and light flavor jet are taken as 0.7, 0.2 and 0.005 respectively [63]. Finally, for an event that contains two boson jet candidates, we proceed with the reconstruction of narrow jets. The constituents of the two boson jet candidates are removed from particle-flow objects of Delphes output. The remnants are clustered using the anti-k_T jet clustering algorithm [68] with a jet cone radius of R = 0.4 and $p_T(j) > 20$ GeV to form narrow jets. The b-tagging is applied to each of the narrow jets with $|\eta(j)| < 2.5$. During the reconstruction, the signal events are required to pass two more preselection cuts: the transverse momenta of two boson jets $p_T(V_1)$, $p_T(V_2) > 200$ GeV and two boson jets should contain either no b-tagged subjet or exactly two b-tagged subjets.

The cross sections of the benchmark points at 14 TeV LHC before and after the preselection are given in Table 2. The Next-to-Leading-Order (NLO) production cross sections of $\tilde{t}_2\bar{\tilde{t}}_2$ plus $\tilde{b}_1\bar{\tilde{b}}_1$ are calculated by Prospino2 [69]. It can be seen that the signal rate decreases dramatically on increasing the particle mass. The preselection efficiencies are around 10%

Table 2 Cross sections of benchmark points before and after preselections at 14 TeV LHC

	$m_{\tilde{t}_2/\tilde{b}_1} \sim 800$ GeV				$m_{\tilde{t}_2/\tilde{b}_1} \sim 1000$ GeV			
	T1BC	T14B	T1BW	T1TN	T1BC	T14B	T1BW	T1TN
$\sigma(\tilde{t}_2\bar{\tilde{t}}_2, \tilde{b}_1\bar{\tilde{b}}_1)$ (NLO) (fb)	99.6	76.5	76.5	76.5	23.0	24.5	24.5	24.5
$\epsilon^{\text{pre}} \times \sigma$ (fb)	6.75	7.47	8.23	7.95	3.02	4.71	4.96	4.76

Table 3 Cross sections of backgrounds before and after preselections at 14 TeV LHC

Process	Total cross section	$\epsilon^{\text{pre}} \times \sigma$ (fb)
$t\bar{t}$	953.6 pb (NNLO) [70]	252.3
$t\bar{t}Z$	1.12 pb (NLO) [71]	6.97
$t\bar{t}W$	769 fb (NLO) [72]	
$t\bar{t}h$	604 fb (NLO) [73]	1.66
tW(+j)	83.6 pb (NNLO) [74]	41.5
WW(+2j)	126 pb(NLO) [75]	203.8
WZ(+2j)	31.9+20.3 pb (NLO) [75]	
ZZ(+2j)	17.7 pb (NLO) [75]	
Wh(+2j)	951+606 fb (NLO) [76]	1.04
Zh(+2j)	880 fb (NLO) [76]	

for benchmark points with $m_{Q_3} = 800\,\text{GeV}$ and become twice larger when $m_{Q_3} = 1\,\text{TeV}$.

We list all possible SM backgrounds for our signal in Table 3, as well as their higher order production cross section at the LHC. After the preselection, the dominant backgrounds are $t\bar{t}$, diboson + jets and tW processes, in which either an energetic top quark or a QCD jet will be mis-tagged as a boson jet in our analysis, and the large missing transverse momentum is mainly due to the existence of a neutrino in the final state.

Comparing Tables 2 and 3, we find that the production rates of our signals are around two orders of magnitude smaller than that of backgrounds after the preselection cuts. Even at the 14 TeV LHC with integrated luminosity of $100\,\text{fb}^{-1}$, the signal significances are only around two. Moreover, because of the smallness of the signal-to-background ratios, the results are quite vulnerable to the systematic uncertainty. We need to apply more refined cuts to obtain a higher signal significance as well as signal-to-background ratio.

First of all, the invariant masses of two boson jets should be close to either of the $W/Z/h$ masses in signal processes. In the top panels of Fig. 5, we plot the distributions of the invariant mass of boson jets (m_{V_1}, m_{V_2}) after pruning [77].[4] In the figure, all backgrounds have been stacked up with a contribution of each process indicated by different colors and the distributions have been normalized to their production cross sections at 14 TeV LHC. We can see that most of signal events have m_{V_1} and m_{V_2} falling between [60, 100] GeV, since the branching ratio to h is suppressed. Meanwhile the backgrounds have relatively flat distribution between [20, 200] GeV, especially for m_{V_1}. This is because of the mis-tagging of the top quark that enhanced the background rate at $m_{V_1} \sim m_t$. It has to be noted that for the benchmark point T1BC $\text{Br}(\tilde{t}_2 \to t\tilde{\chi}_i^0)$ and $\text{Br}(\tilde{b}_1 \to t\tilde{\chi}^{\pm})$ are also sizable. This leads to an enhanced event rate at $m_{V_1} \sim m_t$ as well.

The effective mass for our signal processes,

$$m_{\text{eff}} = \not{E}_T + p_T(V_1) + p_T(V_2) + \sum p_T(\ell) + \sum p_T(j), \tag{3.3}$$

which is correlated with $m_{\tilde{t}_2/\tilde{b}_1}$, should be higher than that for background processes. As shown in the lower-left panel of Fig. 5, the preselection renders the m_{eff} distribution of the background peaks in a wide range between [1000,1200] GeV, while there a large fraction of signal events have $m_{\text{eff}} > 1200$ GeV.

Another useful discriminator that is used frequently in searching supersymmetry is the stransverse mass M_{T_2} [79,80], which could reflect the mass difference between the squark and neutralino in the squark pair production channel with subsequent two body decay $\tilde{q} \to q\tilde{\chi}^0$. By drawing an analogy between our signal process $\tilde{t}_2/\tilde{b} \to V\tilde{t}_1$ and $\tilde{q} \to q\tilde{\chi}^0$, we can define the modified stransverse mass as

$$M_{T_2}(V_1, V_2) = \min_{\mathbf{p}_T^1 + \mathbf{p}_T^2 = \not{\mathbf{p}}_T + \sum \mathbf{p}_T(\ell) + \sum \mathbf{p}_T(j)} \times [\max(m_T(\mathbf{p}(V_1), \mathbf{p}_T^1), m_T(\mathbf{p}(V_2), \mathbf{p}_T^2))], \tag{3.4}$$

where $\sum \mathbf{p}_T(\ell)$ and $\sum \mathbf{p}_T(j)$ are vector sums of the transverse momenta of isolated leptons and narrow jets. The $M_{T_2}(V_1, V_2)$ distribution for signals and backgrounds are presented in the low-right panel of Fig. 4. We can see the signal events are associated to larger values of $M_{T_2}(V_1, V_2)$ than backgrounds events.

In order to obtain better signal and background discrimination, we employ the BDT method that takes into account the distribution profiles of the following variables:

$$p_T(V_1),\ m_{V_1},\ p_T(V_2),\ m_{V_2},\ \not{E}_T,\ m_{\text{eff}},\ M_{T_2}(V_1, V_2). \tag{3.5}$$

[4] The BDRS method uses the filtered mass for the boson jet. But we find that the distribution of the pruned mass has a sharper peak in our case [78].

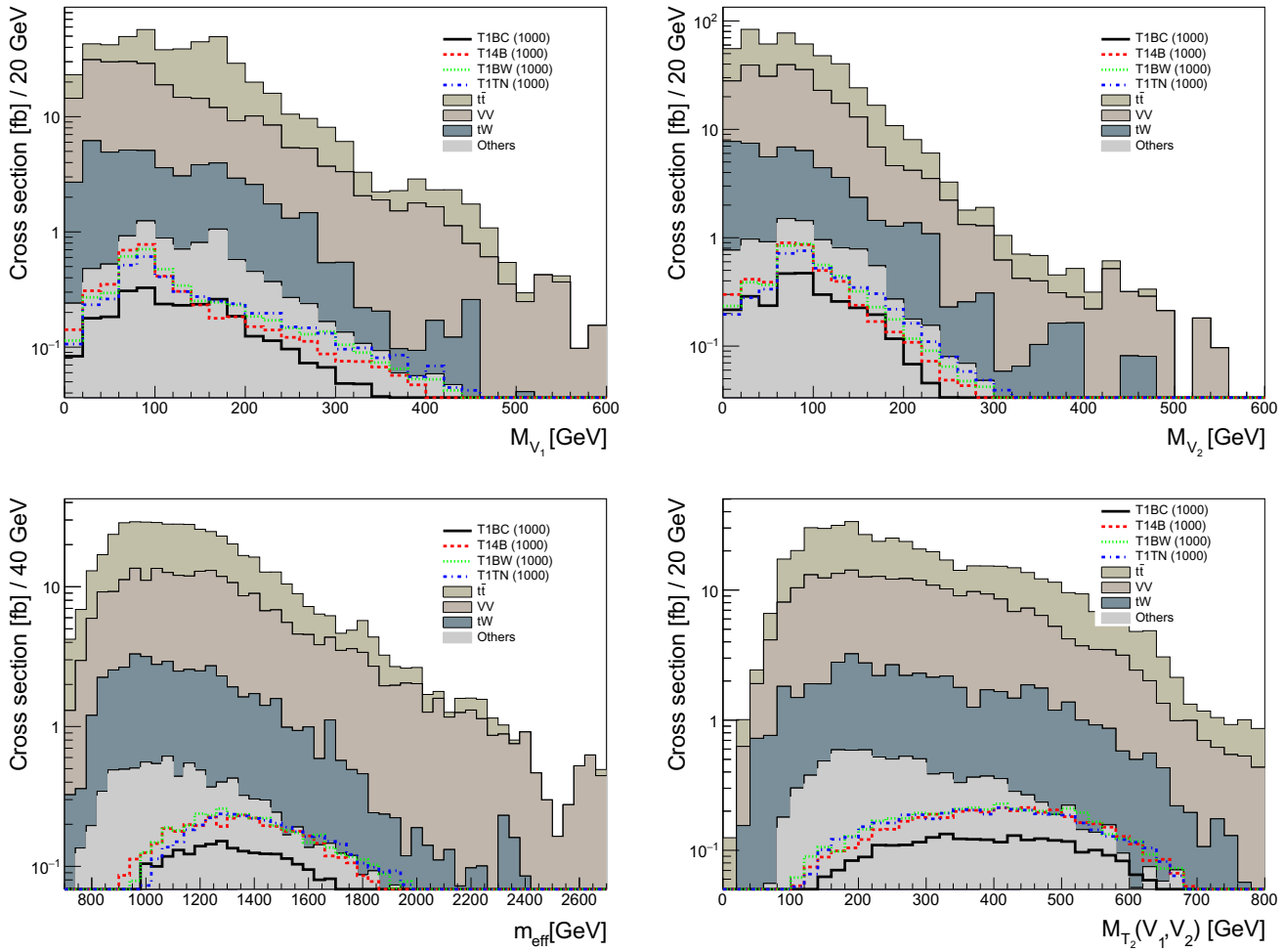

Fig. 4 Kinematic distributions for signals and backgrounds after preselection

Furthermore, the information from the decay products of the light top squark may help to improve our signal identification. So we consider three more variables in the BDT analysis:

$$n_\ell,\ n_b,\ p_T(\ell_1), \tag{3.6}$$

where $p_T(\ell_1)$ is the transverse momentum of the leading lepton if it exists.

The BDT method uses a 100 tree ensemble that requires a minimum training events in each leaf node of 2.5% and a maximum tree depth of two. It is trained on the half of the preselected signal and backgrounds events and is tested on the rest of the events. We also require that the Kolmogorov–Smirnov test of the BDT analysis should be greater than 0.01 to avoid overtraining.

Having the BDT response distributions for both signal and background, we can impose a cut on the BDT responses to improve the signal significance. Figure 5 shows the signal-to-background ratios (left panel) and the signal significances with 100 fb^{-1} data sample (right) for all benchmark points. The signal significance is calculated by

$$\mathcal{S} = \sqrt{2\left((s+b)\ln\left(1+\frac{s}{b}\right)-s\right)}. \tag{3.7}$$

We can see that a cut of BDT $\gtrsim$0.3 will maximize the signal significance and keep the signal-to-background ratio at $\mathcal{O}(10)\%$ level.

In Fig. 6, we plot the signal significances for all benchmark points with different integrated luminosity, where we have chosen the cut BDT $\geq$0.3. A heavier stop sector of $\sim$1 TeV can be excluded at 95% C.L. at very early stage of the LHC run-II. Since the lighter stops $\tilde{t}_1$ of the benchmark points are far beyond the reach of the LHC search at 13 TeV 13.3 fb^{-1}, we conclude that the heavier stop provides a better chance for searching supersymmetry. Moreover, comparing to the method in Ref. [44,46] which utilizes the leptons and b-jets in the final state, our search strategy can achieve a few times larger signal significance because of the higher signal rate.

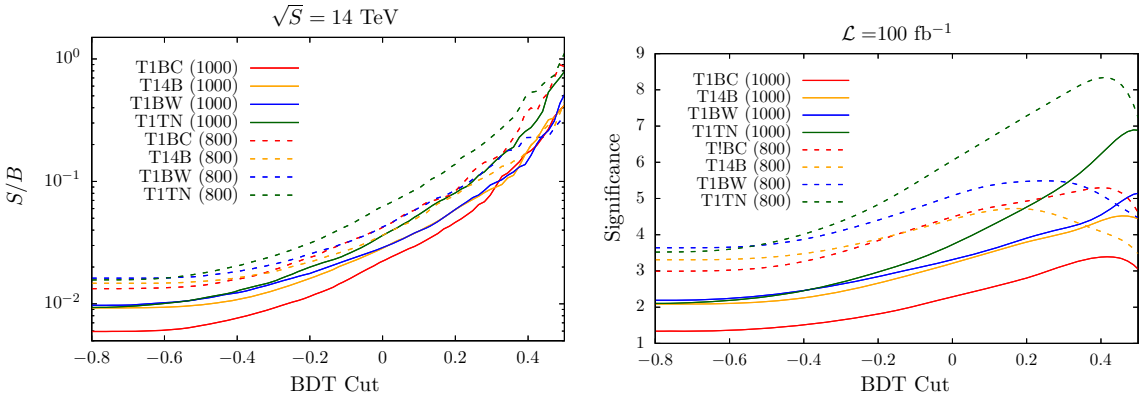

Fig. 5 *Left* the signal-background ratio for varying BDT cut. *Right* the signal significance at integrated luminosity of 100 fb^{-1} for varying BDT cut

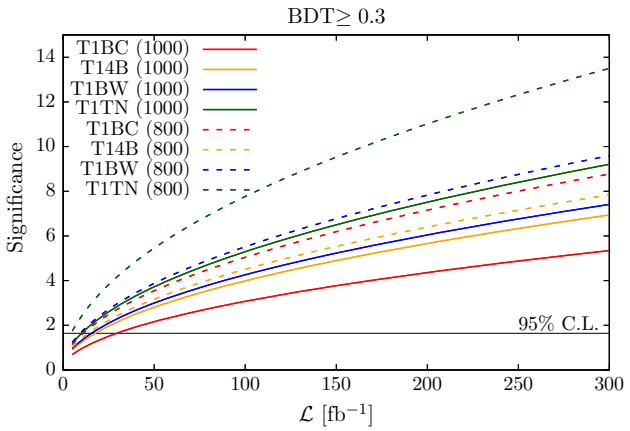

Fig. 6 The signal significance at different integrated luminosities, where the BDT cut is chosen as BDT $\geq$0.3. The horizontal line corresponds to the 95% C.L. exclusion limit

4 Conclusion

A quasi-natural pattern of low energy supersymmetry is considered in this work. The lighter stop is considered to have a mass around a few 100 GeV and to be close to the LSP mass, while the heavier stop and the lighter sbottom have masses around TeV. In this scenario, due to the compressed mass between the lighter stop and the LSP, the lighter stop decay can only produce soft leptons/jets in the final state; thus it evades all current LHC searches and is difficult to probe in future experiments. The heavier stop $\tilde{t}_2$ and lighter sbottom $\tilde{b}_1$, in contrast, may provide a better handle for searching the compressed SUSY.

In the framework of MSSM, considering either the bino or the Higgsino as the LSP, we find that the bosonic modes $h/Z\tilde{t}_1$ ($W\tilde{t}_1$) dominate the $\tilde{t}_2$ ($\tilde{b}_1$) decay in the parameter space with relatively large left–right stop mixing as well as large trilinear coupling A_t. With a moderately large mass gap between the heavier members and lightest stop, the bosons in the decay chain are generically quite energetic. This allows us to employ the jet substructure technique for discriminating the natural SUSY signals in searches at the LHC.

We consider the discovery prospects of eight benchmark points at the LHC-14, in terms of four possible decay modes of the lighter stop $\tilde{t}_1$: (1) $\tilde{t}_1 \to b\tilde{\chi}_1^{\pm}$; (2) $\tilde{t}_1 \to bff\tilde{\chi}_1^0$; (3) $\tilde{t}_1 \to bW\tilde{\chi}_1^0$; (4) $\tilde{t}_1 \to t\tilde{\chi}_1^0$ as well as two different masses of $\tilde{t}_2/\tilde{b}_1$: (a) $m_{\tilde{t}_2/\tilde{b}_1} \sim 800$ GeV; (b) $m_{\tilde{t}_2/\tilde{b}_1} \sim 1000$ GeV. We search for $\tilde{t}_2\bar{\tilde{t}}_2$ and $\tilde{b}_1\bar{\tilde{b}}_1$ production in the final state with two boosted boson jets that have substructures and high invariant masses, leptons/b-jets and MET. After considering background contamination and adopting the BDT method for signal discrimination, we find that a heavier stop and lighter sbottom with masses $\sim$ 1 TeV can be excluded at 95% C.L. with integrated luminosity of 10–30 fb^{-1}. Among the four decay modes of $\tilde{t}_1$, the search sensitivities decrease from $t\tilde{\chi}_1^0$ to $bW\tilde{\chi}_1^0$ to $bff\tilde{\chi}_1^0$, as the mass difference between $\tilde{t}_1$ and $\tilde{\chi}_1^0$ is successively smaller. The $b\tilde{\chi}_1^{\pm}$ mode has the least search sensitivity. This is because this mode is possible only when Higgsino is the LSP. Then the decay branching ratios of $\tilde{t}_2 \to t\tilde{\chi}^0$ / $\tilde{b}_1 \to t\tilde{\chi}^{\pm}$ become competitive to that of the bosonic decay of $\tilde{t}_2$ / $\tilde{b}_1$. Finally, we note that with the aid of the jet substructure and BDT analysis, our search strategy can achieve a few times larger signal significance than the searches proposed in Refs. [44,46], which utilize the multiple leptons and b-jets in the final state.

Acknowledgements This work is supported in part by National Research Foundation of Korea (NRF) Research Grant NRF-2015R1A2A1A05001869 (JL) and IBS under the project code IBS-R018-D1 (MZ).

Funded by SCOAP[3].

References

1. R. Barbieri, G.F. Giudice, Upper bounds on supersymmetric particle masses. Nucl. Phys. B **306**, 63–76 (1988)
2. R. Kitano, Y. Nomura, Supersymmetry, naturalness, and signatures at the LHC. Phys. Rev. D **73**, 095004 (2006). arXiv:hep-ph/0602096
3. G.F. Giudice, R. Rattazzi, Living dangerously with low-energy supersymmetry. Nucl. Phys. B **757**, 19–46 (2006). arXiv:hep-ph/0606105
4. M. Papucci, J.T. Ruderman, A. Weiler, Natural SUSY endures. JHEP **09**, 035 (2012). arXiv:1110.6926
5. ATLAS Collaboration, G. Aad et al., ATLAS Run 1 searches for direct pair production of third-generation squarks at the Large Hadron Collider. Eur. Phys. J. C **75**(10), 510 (2015). arXiv:1506.08616. [Erratum: Eur. Phys. J.C76,no.3,153(2016)]
6. ATLAS Collaboration, M. Aaboud et al., Search for new phenomena in final states with an energetic jet and large missing transverse momentum in pp collisions at $\sqrt{s} = 13$ TeV using the ATLAS detector. Phys. Rev. D **94**(3), 032005 (2016). arXiv:1604.07773
7. ATLAS Collaboration, Search for direct top squark pair production and dark matter production in final states with two leptons in $\sqrt{s} =$ 13 TeV pp collisions using 13.3 fb $^{-1}$ of ATLAS data. ATLAS-CONF-2016-076 (2016)
8. ATLAS Collaboration, Search for top squarks in final states with one isolated lepton, jets, and missing transverse momentum in $\sqrt{s}$ = 13 TeV pp collisions with the ATLAS detector. ATLAS-CONF-2016-050 (2016)
9. ATLAS Collaboration, Search for the supersymmetric partner of the top quark in the Jets+Emiss final state at sqrt(s) = 13 TeV. ATLAS-CONF-2016-077 (2016)
10. CMS Collaboration, Search for direct top squark pair production in the single lepton final state at $\sqrt{s} = 13$ TeV. CMS-PAS-SUS-16-028 (2016)
11. CMS Collaboration, Search for direct top squark pair production in the fully hadronic final state in proton-proton collisions at sqrt(s) = 13 TeV corresponding to an integrated luminosity of 12.9/fb. CMS-PAS-SUS-16-029 (2016)
12. CMS Collaboration, Search for supersymmetry in the all-hadronic final state using top quark tagging in pp collisions at sqrt(s) = 13 TeV. CMS-PAS-SUS-16-030 (2016)
13. M. Carena, A. Freitas, C.E.M. Wagner, Light stop searches at the LHC in events with one hard photon or jet and missing energy. JHEP **10**, 109 (2008). arXiv:0808.2298
14. S. Bornhauser, M. Drees, S. Grab, J.S. Kim, Light stop searches at the LHC in events with two b-jets and missing energy. Phys. Rev. D **83**, 035008 (2011). arXiv:1011.5508
15. M.A. Ajaib, T. Li, Q. Shafi, Stop-neutralino coannihilation in the light of LHC. Phys. Rev. D **85**, 055021 (2012). arXiv:1111.4467
16. Z. Han, A. Katz, D. Krohn, M. Reece, (Light) Stop signs. JHEP **08**, 083 (2012). arXiv:1205.5808
17. M. Drees, M. Hanussek, J.S. Kim, Light stop searches at the LHC with monojet events. Phys. Rev. D **86**, 035024 (2012). arXiv:1201.5714
18. J. Cao, C. Han, L. Wu, J.M. Yang, Y. Zhang, Probing natural SUSY from stop pair production at the LHC. JHEP **11**, 039 (2012). arXiv:1206.3865
19. Z.-H. Yu, X.-J. Bi, Q.-S. Yan, P.-F. Yin, Detecting light stop pairs in coannihilation scenarios at the LHC. Phys. Rev. D **87**(5), 055007 (2013). arXiv:1211.2997
20. K. Krizka, A. Kumar, D.E. Morrissey, Very light scalar top quarks at the LHC. Phys. Rev. D **87**(9), 095016 (2013). arXiv:1212.4856
21. A. Delgado, G.F. Giudice, G. Isidori, M. Pierini, A. Strumia, The light stop window. Eur. Phys. J. C **73**(3), 2370 (2013). arXiv:1212.6847
22. C. Han, K.-I. Hikasa, L. Wu, J.M. Yang, Y. Zhang, Current experimental bounds on stop mass in natural SUSY. JHEP **10**, 216 (2013). arXiv:1308.5307
23. M. Czakon, A. Mitov, M. Papucci, J.T. Ruderman, A. Weiler, Closing the stop gap. Phys. Rev. Lett. **113**(20), 201803 (2014). arXiv:1407.1043
24. G. Belanger, D. Ghosh, R. Godbole, M. Guchait, D. Sengupta, Probing the flavor violating scalar top quark signal at the LHC. Phys. Rev. D **89**, 015003 (2014). arXiv:1308.6484
25. B. Dutta, W. Flanagan, A. Gurrola, W. Johns, T. Kamon, P. Sheldon, K. Sinha, K. Wang, S. Wu, Probing compressed top squark scenarios at the LHC at 14 TeV. Phys. Rev. D **90**(9), 095022 (2014). arXiv:1312.1348
26. R. Grber, M.M. Mhlleitner, E. Popenda, A. Wlotzka, Light stop decays: implications for LHC searches. Eur. Phys. J. C **75**, 420 (2015). arXiv:1408.4662
27. K-i Hikasa, J. Li, L. Wu, J.M. Yang, Single top squark production as a probe of natural supersymmetry at the LHC. Phys. Rev. D **93**(3), 035003 (2016). arXiv:1505.06006
28. H. An, L.-T. Wang, Opening up the compressed region of top squark searches at 13 TeV LHC. Phys. Rev. Lett. **115**, 181602 (2015). arXiv:1506.00653
29. G. Belanger, D. Ghosh, R. Godbole, S. Kulkarni, Light stop in the MSSM after LHC Run 1. JHEP **09**, 214 (2015). arXiv:1506.00665
30. A. Kobakhidze, N. Liu, L. Wu, J.M. Yang, M. Zhang, Closing up a light stop window in natural SUSY at LHC. Phys. Lett. B **755**, 76–81 (2016). arXiv:1511.02371
31. G. Ferretti, R. Franceschini, C. Petersson, R. Torre, Spot the stop with a b-tag. Phys. Rev. Lett. **114**, 201801 (2015). arXiv:1502.01721
32. S. Macaluso, M. Park, D. Shih, B. Tweedie, Revealing compressed stops using high-momentum recoils. JHEP **03**, 151 (2016). arXiv:1506.07885
33. D. Goncalves, K. Sakurai, M. Takeuchi, Tagging a monotop signature in natural SUSY. Phys. Rev. D **95**(1), 015030 (2017). arXiv:1610.06179
34. H.-C. Cheng, C. Gao, L. Li, N.A. Neill, Stop search in the compressed region via semileptonic decays. JHEP **05**, 036 (2016). arXiv:1604.00007
35. B. Kaufman, P. Nath, B.D. Nelson, A.B. Spisak, Light stops and observation of supersymmetry at LHC RUN-II. Phys. Rev. D **92**, 095021 (2015). arXiv:1509.02530
36. G.H. Duan, K.-I. Hikasa, L. Wu, J.M. Yang, M. Zhang, Leptonic mono-top from single stop production at the LHC. JHEP **03**, 091 (2017). arXiv:1611.05211
37. C. Han, J. Ren, L. Wu, J.M. Yang, M. Zhang, Top-squark in natural SUSY under current LHC run-2 data. Eur. Phys. J. C **77**(2), 93 (2017). arXiv:1609.02361
38. D. Gonalves, K. Sakurai, M. Takeuchi, Mono-top signature from supersymmetric $t\bar{t}H$ channel. Phys. Rev. D **94**(7), 075009 (2016). arXiv:1604.03938
39. J. Guo, Z. Kang, J. Li, T. Li, Y. Liu, Simplified supersymmetry with sneutrino LSP at 8 TeV LHC. JHEP **10**, 164 (2014). arXiv:1312.2821
40. ATLAS Collaboration, G. Aad et al., Search for direct top squark pair production in events with a Z boson, b-jets and missing transverse momentum in sqrt(s)=8 TeV pp collisions with the ATLAS detector. Eur. Phys. J. C **74**(6), 2883 (2014). arXiv:1403.5222
41. C.M.S. Collaboration, V. Khachatryan et al., Search for top-squark pairs decaying into Higgs or Z bosons in pp collisions at $\sqrt{s}$ =8 TeV. Phys. Lett. B **736**, 371–397 (2014). arXiv:1405.3886

42. J. Guo, Z. Kang, J. Li, T. Li, Implications of Higgs sterility for the Higgs and stop sectors. arXiv:1308.3075
43. J. Beuria, A. Chatterjee, A. Datta, S.K. Rai, Two light stops in the NMSSM and the LHC. JHEP **09**, 073 (2015). arXiv:1505.00604
44. H.-C. Cheng, L. Li, Q. Qin, Second stop and sbottom searches with a stealth stop. JHEP **11**, 181 (2016). arXiv:1607.06547
45. H. An, J. Gu, L.-T. Wang, Exploring the nearly degenerate stop region with sbottom decays. arXiv:1611.09868
46. A. Pierce, B. Shakya, Implications of a stop sector signal at the LHC. arXiv:1611.00771
47. J.M. Butterworth, A.R. Davison, M. Rubin, G.P. Salam, Jet substructure as a new Higgs search channel at the LHC. Phys. Rev. Lett. **100**, 242001 (2008). arXiv:0802.2470
48. D.E. Kaplan, K. Rehermann, M.D. Schwartz, B. Tweedie, Top tagging: a method for identifying boosted hadronically decaying top quarks. Phys. Rev. Lett. **101**, 142001 (2008). arXiv:0806.0848
49. T. Plehn, G.P. Salam, M. Spannowsky, Fat jets for a light Higgs. Phys. Rev. Lett. **104**, 111801 (2010). arXiv:0910.5472
50. Y. Cui, Z. Han, M.D. Schwartz, W-jet tagging: optimizing the identification of boosted hadronically-decaying W bosons. Phys. Rev. D **83**, 074023 (2011). arXiv:1012.2077
51. D. Ghosh, Boosted dibosons from mixed heavy top squarks. Phys. Rev. D **88**(11), 115013 (2013). arXiv:1308.0320
52. Z. Kang, J. Li, T. Li, On naturalness of the MSSM and NMSSM. JHEP **11**, 024 (2012). arXiv:1201.5305
53. J.-J. Cao, Z.-X. Heng, J.M. Yang, Y.-M. Zhang, J.-Y. Zhu, A SM-like Higgs near 125 GeV in low energy SUSY: a comparative study for MSSM and NMSSM. JHEP **03**, 086 (2012). arXiv:1202.5821
54. Z. Kang, T. Li, T. Liu, C. Tong, J.M. Yang, A heavy SM-like Higgs and a light stop from Yukawa-deflected gauge mediation. Phys. Rev. D **86**, 095020 (2012). arXiv:1203.2336
55. J.R. Ellis, K.A. Olive, Y. Santoso, Calculations of neutralino stop coannihilation in the CMSSM. Astropart. Phys. **18**, 395–432 (2003). arXiv:hep-ph/0112113
56. A. Bartl, W. Majerotto, W. Porod, Squark and gluino decays for large tan β. Zeitschrift für Physik C Part. Fields **64**(3), 499–507 (1994)
57. Z. Kang, P. Ko, J. Li, New physics opportunities in the boosted di-Higgs-boson plus missing transverse energy signature. Phys. Rev. Lett. **116**(13), 131801 (2016). arXiv:1504.04128
58. A. Djouadi, J.-L. Kneur, G. Moultaka, SuSpect: a Fortran code for the supersymmetric and Higgs particle spectrum in the MSSM. Comput. Phys. Commun. **176**, 426–455 (2007). arXiv:hep-ph/0211331
59. A. Djouadi, M. Muhlleitner, M. Spira, Acta Phys. Polon. B **38**, 635–644 (2007). arXiv:hep-ph/0609292
60. J. Alwall, R. Frederix, S. Frixione, V. Hirschi, F. Maltoni, O. Mattelaer, H.S. Shao, T. Stelzer, P. Torrielli, M. Zaro, The automated computation of tree-level and next-to-leading order differential cross sections, and their matching to parton shower simulations. JHEP **07**, 079 (2014). arXiv:1405.0301
61. T. Sjostrand, S. Mrenna, P.Z. Skands, PYTHIA 6.4 physics and manual. JHEP **05**, 026 (2006). arXiv:hep-ph/0603175
62. DELPHES 3 Collaboration, J. de Favereau, C. Delaere, P. Demin, A. Giammanco, V. Lemaître, A. Mertens, M. Selvaggi, DELPHES 3, A modular framework for fast simulation of a generic collider experiment. JHEP **02**, 057 (2014). arXiv:1307.6346
63. ATLAS Collaboration, G. Aad et al., Performance of b-Jet identification in the ATLAS experiment. JINST **11**(04), P04008 (2016). arXiv:1512.01094
64. A. Altheimer et al., Boosted objects and jet substructure at the LHC. Report of BOOST2012, held at IFIC Valencia, 23rd–27th of July 2012. Eur. Phys. J. C **74**(3), 2792 (2014). arXiv:1311.2708
65. V. Rentala, W. Shepherd, T.M.P. Tait, Tagging boosted Ws with wavelets. JHEP **08**, 042 (2014). arXiv:1404.1929
66. M. Cacciari, G.P. Salam, G. Soyez, FastJet user manual. Eur. Phys. J. C **72**, 1896 (2012). arXiv:1111.6097
67. Y.L. Dokshitzer, G.D. Leder, S. Moretti, B.R. Webber, Better jet clustering algorithms. JHEP **08**, 001 (1997). arXiv:hep-ph/9707323
68. M. Cacciari, G.P. Salam, G. Soyez, The Anti-k(t) jet clustering algorithm. JHEP **04**, 063 (2008). arXiv:0802.1189
69. W. Beenakker, M. Kramer, T. Plehn, M. Spira, P.M. Zerwas, Stop production at hadron colliders. Nucl. Phys. B **515**, 3–14 (1998). arXiv:hep-ph/9710451
70. M. Czakon, P. Fiedler, A. Mitov, Total top-quark pair-production cross section at hadron colliders through $O(\frac{4}{S})$. Phys. Rev. Lett. **110**, 252004 (2013). arXiv:1303.6254
71. A. Kardos, Z. Trocsanyi, C. Papadopoulos, Top quark pair production in association with a Z-boson at NLO accuracy. Phys. Rev. D **85**, 054015 (2012). arXiv:1111.0610
72. J.M. Campbell, R.K. Ellis, $t\bar{t}W^{+-}$ production and decay at NLO. JHEP **07**, 052 (2012). arXiv:1204.5678
73. LHC Higgs Cross Section Working Group Collaboration, J.R. Andersen et al., Handbook of LHC Higgs cross sections: 3. Higgs properties. arXiv:1307.1347
74. N. Kidonakis, Top quark production, in *Proceedings, Helmholtz International Summer School on Physics of Heavy Quarks and Hadrons (HQ 2013): JINR, Dubna, Russia*, July 15–28, 2013 (2014), pp. 139–168. arXiv:1311.0283
75. J.M. Campbell, R.K. Ellis, C. Williams, Vector boson pair production at the LHC. JHEP **07**, 018 (2011). arXiv:1105.0020
76. J.M. Campbell, R.K. Ellis, C. Williams, Associated production of a Higgs boson at NNLO. JHEP **06**, 179 (2016). arXiv:1601.00658
77. S.D. Ellis, C.K. Vermilion, J.R. Walsh, Recombination algorithms and jet substructure: pruning as a tool for heavy particle searches. Phys. Rev. D **81**, 094023 (2010). arXiv:0912.0033
78. ATLAS Collaboration, G. Aad et al. Performance of jet substructure techniques for large-R jets in proton-proton collisions at $\sqrt{s}$ = 7 TeV using the ATLAS detector. JHEP **09** (2013) 076, arXiv:1306.4945
79. C.G. Lester, D.J. Summers, Measuring masses of semiinvisibly decaying particles pair produced at hadron colliders. Phys. Lett. B **463**, 99–103 (1999). arXiv:hep-ph/9906349
80. A. Barr, C. Lester, P. Stephens, m(T2): the truth behind the glamour. J. Phys. G **29**, 2343–2363 (2003). arXiv:hep-ph/0304226